Infiltration processes in karst using an event-based conceptual model of flow and transport of dissolved organic carbon

Jean-Baptiste Charlier, Jacques Mudry, Catherine Bertrand

Infiltration processes in karst using an event-based conceptual model of flow and transport of dissolved organic carbon

Jean-Baptiste Charlier*, Jacques Mudry & Catherine Bertrand

UMR Chrono-Environment – University of Franche-Comté, 16 route de Gray, F-25030 Besançon, France.
* corresponding author: E-mail: jb.charlier@gmail.com.

Abstract

The aim of this study is to characterize karst infiltration processes during flood events using a rainfall-discharge model coupled with a transport model for non-conservative solutes. The modelling approach is based on a classical karst devoted model with three connected reservoirs: SOIL (and epikarst) that feeds the aquifer partitioned into DIFFUSE and CONDUIT. Solute transport is modelled using mixing equations, including an empirical retardation factor in SOIL, as well as a first order solute decay. In order to take into account some specificities commonly observed in karst systems, three parameters are added to simulate overflows, piston-type flows in conduits, and a variation of the recharge area according to the initial hydrological conditions. To validate our approach, we used the dissolved organic carbon (DOC) as tracer, which is a non-conservative compound derived from the enrichment of infiltrated water into soil humic substances. The model was applied on a small karst system at Fertans in the French Jura mountains, where discharge and continuous measurements of DOC fluorescence are recorded. The model was calibrated and validated on a set of 19 flood events, showing that the model adequately simulated hydrographs and delayed chemographs during flood events with various rainfall intensities. A large variability of the recharge area was highlighted according to low and high groundwater level periods, and was attributed to the state of hydraulic connectivity in the unsaturated zone. The model simulate the contributions of pre-event and event waters during flood events and allow to better quantify the available resource considering the mixing effect of DOC. It shows, in particular, that total discharge of some flood events during dry periods are mainly composed by pre-event water via piston flow-type processes. Finally, this study show the ability of mixing model to properly simulate solute transport taking into account degradation and retardation processes.

1. Introduction

Due to their strong heterogeneity, hydrological modelling of karst systems is often based upon conceptual models generally lumped at the catchment scale (e.g. recently RIMMER & SALINGAR, 2006; TRITZ et al., 2011). These models calibrated only on hydrographs are able to simulate discharge with good performances, but are not necessarily able to simulate hydrochemistry, which is commonly used to establish the hydrodynamic function of the studied systems (see HUNKELER & MUDRY (2007) for a review). To date, the use of natural tracers is an efficient indirect means to gain additional insight into the hydrological functioning, but is still qualitative. Consequently, hydrochemistry appears to be a powerful additional tool to constrain conceptual hydrological models during flood events by simulating tracers of short transit time, i.e. non-conservative tracers.

In this framework, the aim of this study is to characterize karst infiltration processes during flood events using an hydrodynamic conceptual model coupled with a transport model for non-conservative tracers. The tracer used to validate this model is the dissolved organic carbon (DOC), which is originated from soil cover and is recognized as a pertinent tracer of short transit time (e.g. EMBLANCH et al., 1998; PRONK et al., 2006). The model is applied on a small site in the French Jura at Fertans where DOC peak is delayed from peakflows (CHARLIER et al., 2010). Since the monitoring of spring discharge and DOC were continuous (using a field fluorometer for DOC (SCHNEGG, 2003)), the challenge was to simulate hydrograph and delayed chemograph at a hourly time step. We present in this paper simulations results carried out at the flood event time scale when diffuse and localised infiltrations occur simultaneously.

2. Study site

2.1. Hydrogeological framework

The experimental site of Fertans (47°03'21"N, 06°03'51"E) is located in the French Jura mountains (Fig. 1). Fertans is at 530m ASL on a carbonate plateau delimited by valleys of 150m depth. Karstic landforms are visible on the plateau: dolines, karren zones, dry valley, which suggest that karstification is relatively high in the study zone. The plateau is drained by contact springs located at the base of the cliffs.

The climate is oceanic with a high mountainous influence given annual rainfall of around 1300mm. The geological formations of the Amancey plateau are tabular and composed of compact limestones on marl and marly-calcareous of Oxfordian age (Fig. 1). The soil is a leptosol of around 15 cm depth, and covered mainly by grassland and hardwood.

2.2. Monitoring sites

Measurements were conducted from 01 July 2009 to 05 May 2010. Hourly rainfall and air temperature were recorded by METEO France at Coulans-sur-Lison at Eternoz (47°01'04"N, 06°01'02"E, 468m ASL), located 9km SW of the experimental site of Fertans. Monthly potential evapotranspiration (PET) was calculated according to Thornthwaite's formula.

The DOC signal in infiltrated water was measured using rainfall simulations above a lysimeter located at 20cm below the soil cover, in a grassland in the supposed recharge area. Distilled water was used for this experiment, and DOC in the collected drainage water was measured using a Shimadzu 5050 carbon analyser.

A small spring was monitored at the base of the Fertans cliff at an elevation of 500m ASL. The unsaturated zone of the system is composed of a 25m-depth fractured compact limestone. The recharge area A is estimated to be 0.45km², according to the annual water balance. Discharge and continuous DOC measurements were carried out every 15 minutes. Continuous DOC measurements were estimated from natural fluorescence measurements using a field fluorometer (SCHNEGG, 2003).

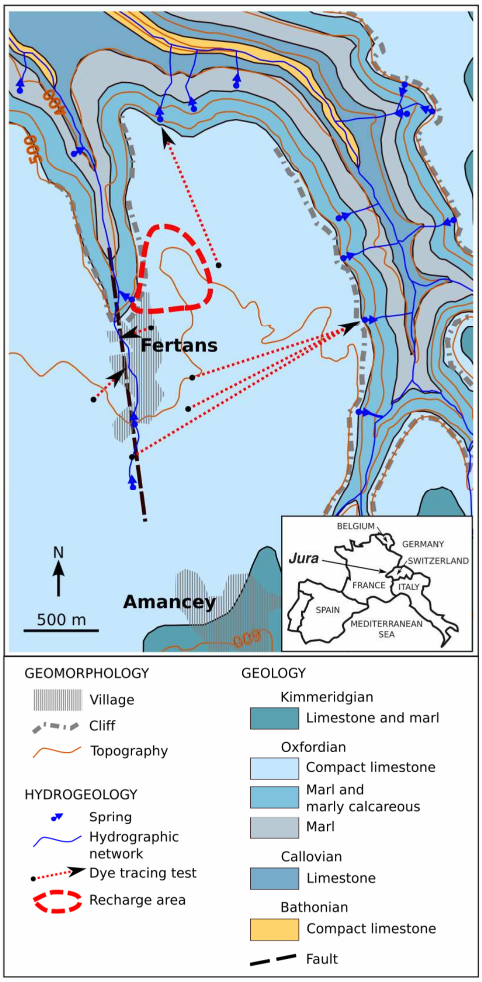

Figure 1: Hydrogeological framework of the Fertans site; Geological map adapted from BRGM (1975).

2.3. Characteristics of flood events

To study the hydrological response of the karstic system after rainfall, we applied the model at the event time scale. Nineteen flood events were selected with a rainfall depth ranging between 7 and 41.1mm, and a DOC transport ranging between 0.7 and 28.3kg.

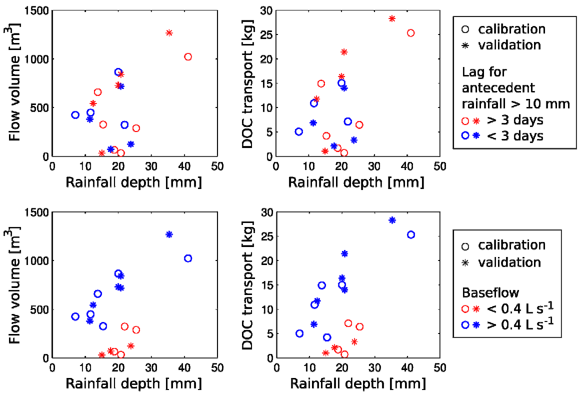

Figure 2: Flood events characteristics showing flow volume and DOC transport vs. rainfall depth, in terms of two hydric initial conditions: the lag time for antecedent rainfall above 10mm (top), and the baseflow (bottom).

Figure 2 presents the response of the system for flows and transport vs. rainfall depth for the selected flood events. Two types of initial hydric conditions were tested to identify groups: i) the lag time for antecedent rainfall depth greater than 10mm (below or above 3 days), which is an indicator of the soil saturation state, and ii) the initial discharge or baseflow (below or above $0.4 L.s^{-1}$), which is an indicator of the initial groundwater level in the system. First, according to the antecedent rainfall depth, no influence was observed on the system response. Then, according to the baseflow, we observe a large gap of the system response between a low and a higher level. For a same rainfall depth between 15 to 25 mm, the flow volume is at the minimum 3-fold higher in high water level periods. This result showed that the variability of the hydrological response at Fertans is not controlled by the soil saturation state, as commonly observed in catchment hydrology. But, that this is mainly controlled by the initial groundwater level. Therefore, we assume that the variability of the hydrological reponse was due to a variation of the recharge area, i.e. by a smallest recharge area during low baseflow periods.

3. Modelling approach

3.1. Basic model

The model used is presented in Figure 3. It is designed to simulate discharge and concentration of a non-conservative tracer during flood events at the spring of a karst system. The model is based on a classical karst model with 3 connected reservoirs: SOIL that feeds the aquifer partitioned into DIFFUSE and CONDUIT reservoir. Such model-type was recently tested by Fleury et al. (2007) and by Moussu et al. (2011). The temporal change of concentration of substances dissolved in a reservoir is simulated using a mixing model including degradation. The degradation rate (λ) is based on a linear law, allowing to express λ as a function of the half-life (*DT50*) of the solute element ($\lambda = 0.693/\mathrm{DT50}$). In order to take into account of the retardation factor of the solute (i.e. the delay generated partly by sorption processes), we added a DELAY reservoir below the SOIL reservoir (see Fig. 3). This DELAY reservoir concerns solute transport only, buffering the solute velocity compared to the water velocity.

3.2. Extended version of the model taking into account specificities of the study site

Three parameters were added to the basic model structure presented above in order to take into account some specificities commonly observed in karst systems as in the study site (Fig. 3): V_{PISTON}, $Q_{overflow}$, and *alpha*.

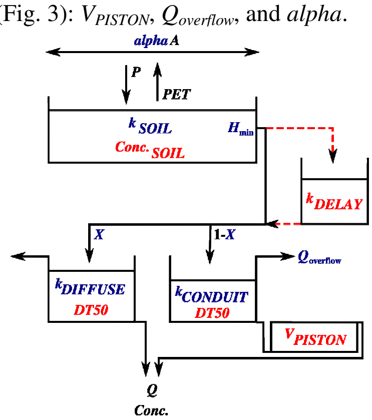

Figure 3: Structure of the conceptual model showing flow parameters in blue and tracer parameters in red (each parameter signification is detailed in Table 1).

A volume of water stored called V_{PISTON}, was added to simulate the arrival of pre-event water (i.e. water initially stored in the system drained by piston-type flow) before the arrival of event water (i.e. recent infiltrated rainwater). This storage has a siphon structure downstream the CONDUIT, and is drained at the beginning of the event without dilution by water in the CONDUIT.

The overflow parameter $Q_{overflow}$ is justified from hydrograph analysis of the Fertans spring, and may be linked to observations made on the field nearby the spring, where some small fracture springs are flowing only after heavy rainfall events.

The variability of the recharge area is simply controlled by *alpha* as a factor of the maximum recharge area *A*.

3.3. Parameterization

The model runs on a hourly time step. The extended version of the model needs a total of 11 parameters that may be fixed or calibrated. They are summarized in Fig. 3 and Table 1. Four of these parameters have been estimated: $k_{DIFFUSE}$, $k_{CONDUIT}$ and $Q_{overflow}$ using hydrograph analysis, and *DT50* from laboratory experiment carried out by Batiot (2002). Finally, there are seven parameters that need to be calibrated: *alpha*, k_{SOIL}, $H_{min,\ SOIL}$, *X*, V_{PISTON}, $Conc._{SOIL}$, and k_{DELAY}.

Name	Reservoir	Signification	Calibration value**
alpha*	all	Contribution of the recharge area	7% (low) or 100% (high)
k_{SOIL}*	SOIL	Recession coefficent	0.3 (low) or 0.09 (high)
$H_{min,\ SOIL}$*	SOIL	Minimum storage for recharge	14 mm
X*	DIFFUSE & CONDUIT	Partition coefficient	41% for DIFFUSE
$k_{DIFFUSE}$	DIFFUSE	Recession coefficient	0.03
$k_{CONDUIT}$	CONDUIT	Recession coefficient	0.70
V_{PISTON}*	PISTON	Total volume	10 (low) 200 (high)
$Q_{overflow}$	DIFFUSE & CONDUIT	Maximum spring discharge due to overflow	4.9 L s^{-1}
$Conc._{SOIL}$ *	DIFFUSE & CONDUIT	Tracer concentration from SOIL	18 mg L^{-1}
DT50	DIFFUSE & CONDUIT	Half-life of the tracer	9 days
k_{DELAY}*	DELAY	Recession coefficient	0.70

Table 1: Parameter description.
** indicates the calibrated parameters; ** when low and high conditions are indicated, it refers to baseflow <0.4 and ≥0.4L*

The model inputs are the rainfall and PET, and the outputs are a simulated hydrograph and chemograph, which were compared to the observed ones to test model performances. For model initialization, initial SOIL storage is estimated according antecedent rainfall, initial DIFFUSE storage is calculated from baseflow value, and initial CONDUIT storage is equal to zero.

The nineteen flood events were split at random between a set of 10 events for calibration and a set of 9 events for validation. A collective calibration procedure was carried out on the calibration set: i) an optimisation of the discharge simulation using the Nash-Sutcliffe's coefficient of efficiency NS, and ii) an optimisation of the chemograph simulation using the determination coefficient R^2.

A low and a high groundwater level were considered for simulation, corresponding to baseflow inferior or superior to $0.4 L.s^{-1}$, respectively. Only *alpha*, k_{SOIL}, and V_{PISTON} were identified as significantly different between these two periods.

4. Results

4.1. Model application on Fertans spring

For calibration and validation sets, NS criterion on discharge was 0.86 and 0.85, respectively, and R^2 criterion on DOC fluctuations was 0.4 and 0.36, respectively. These results showed that the model adequately simulated hydrographs and delayed chemographs during flood events with various rainfall intensities and various antecedent hydrological conditions. Two simulation examples are presented in Fig. 4 showing the good fit between simulated and observed discharge as well as DOC concentration, for low and high groundwater level periods.

4.2. Hydrogeological behaviour

Parameter calibration values are given in Table 1. We aim in this paragraph to design a hydrogeological conceptual model of Fertans spring from the analysis of the main parameters.

Regarding contributions between DIFFUSE and CONDUIT reservoirs (*X* parameter), the model shows that around 41% of the recharge (effective rainfall) is infiltrated fast via the conduit network. Thus, we may suppose that 59% of the recharge contributed to the water storage of the system.

The simulated recharge area is varying from 7% to 100% regarding *alpha* parameter, meaning that in high groundwater level periods there is a better hydraulic connectivity in conduits in all the unsaturated zone. This explanation is highly justified in karst hydrology where surface and groundwater interbasin flows depends on the hydraulic connectivity state (Bailly-Comte et al., 2009).

The simulated contribution of pre-event water (V_{PISTON} parameter) during flood events varied greatly according to low and high groundwater level periods. To illustrate this variability, two representative examples are given in Fig. 4. For the event in a wet period (bottom of Fig. 4), pre-event water represents 20% of total flow volume before the DOC peak generated by the arrival of rainwater in conduits. In this case, piston-type flows are a minor process compared to fast infiltration in conduits. For the event in a dry period (top of Fig. 4), the DOC signal remains flat due to a contribution of pre-event water only. In this last case, flood event is generated by piston-type flows without dilution effect by infiltrated rainwater.

Concerning DOC transport, this modelling approach show the availability for mixing models to properly simulate transport of non-conservative solutes. A first-order degradation rate as a function of the half-life *DT50* appears to be adapted to simulations at the flood event time scale. Regarding the empirical retardation factor (k_{DELAY}) added for the tracer at the output of SOIL reservoir, simulations showed that the retardation processes, due mainly to sorption mechanisms notably in the soil cover, play a significative role for solute transfer. Finally, regarding DOC concentration from soil cover, the simulated concentration ($Conc._{SOIL}$ = $18 mg.L^{-1}$) is in the same range than the measured concentration in drainage water ($10 mg.L^{-1}$).

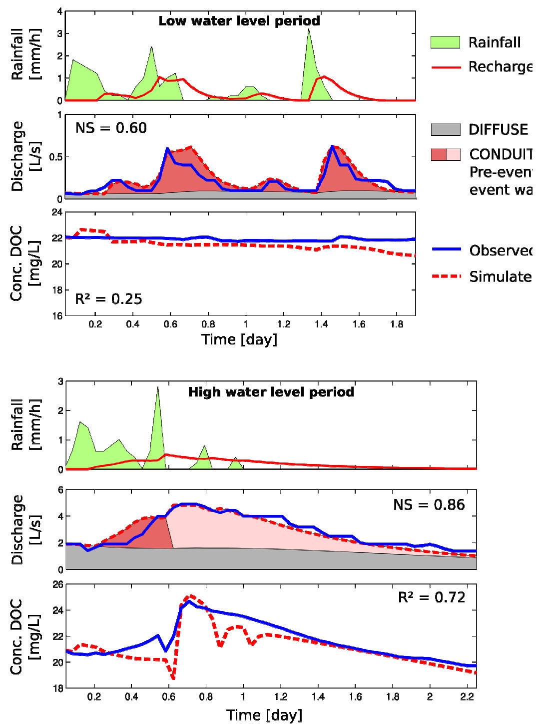

Figure 4: Simulation example for two events in low (top) and high (bottom) groundwater level periods.

5. Conclusion

In this study, we assumed that coupling tracer transport in hydrological conceptual model would be a pertinent tool to constrain karst infiltration models. We validate our approach using continuous DOC signal as tracer of infiltration in a small spring. On the basis of the simulations results, an hydrogeological model was designed. First, after rainfall events, we showed that 41% of the recharge water is infiltrated fast via conduit network. Then, a strong variability of the system response was highlighted according to low and high groundwater level periods. This pattern was attributed to a variability of the recharge area due to the state of hydraulic connectivity in the unsaturated zone. Moreover, pre-event and event waters varied greatly according to this hydrological conditions. Consequently, fast infiltration of event water appears to be the main process during high groundwater level periods, whereas pre-event water by piston-type flows can generate up to the total flow volume during low groundwater leval periods. Finally, this study shows the ability of mixing model to properly simulate solute transport taking into account degradation and retardation processes.

References

Bailly-Comte, V., Jourde, H., & Pistre, S., 2009. Conceptualization and classification of groundwater–surface water hydrodynamic interactions in karst watersheds: case of the karst watershed of the Coulazou River (Southern France). *Journal of Hydrology*, 376:456–462.

Batiot, C., 2002. Étude expérimentale du cycle du carbone en régions karstiques. Apport du carbone organique et du carbone minéral à la connaissance hydrogéologique des systèmes. PhD thesis, University of Avignon, Avignon, France.

BRGM, 1975. Geological map of Quingey at 1:50000 scale, 529, BRGM (ed), Orléans, France.

Charlier, J.-B., Mudry J., & Bertrand C., 2010. Use of dissolved organic carbon to characterize infiltration in a small karst system in the French Jura mountains (Fertans, France). In Andreo B. et al. (Eds), Advances in research in karst media. Berlin : Springer, 2010. p 151-156.

Emblanch C., Blavoux B., Puig J. M., & Mudry J., 1998. Dissolved organic carbon of infiltration within the autogenic karst hydrosystem, *Geophysical Research Letters*, 25(9): 1459– 1462.

Fleury P., Plagnes V., & Bakalowicz M., 2007. Modelling of the functioning of karst aquifers with a reservoir model: Application to Fontaine de Vaucluse (South of France). *Journal of Hydrology*, 345: 38-49.

Hunkeler D., & Mudry J., 2007. Hydrochemical methods. In Goldscheider N. & Drew D. (Eds), Methods in karst hydrogeology. Taylor & Francis, London. International Contributions to Hydrogeology, 26: 93-121.

Moussu F., Oudin L., Plagnes V., Mangin A., & Bendjoudi H., 2011. A multi-objective calibration framework for rainfall–discharge models applied to karst systems, *Journal of Hydrology*, 400: 364-376.

Pronk M., Goldscheider N., & Zopfi J., 2006. Dynamics and interaction of organic carbon, turbidity and bacteria in a karst aquifer system, *Hydrogeology Journal*, 14: 473-484.

Rimmer A., & Salingar Y., 2006. Modelling precipitation-streamflow processes in karst basin: The case of the Jordan River sources, Israel. *Journal of Hydrology*, 331: 524-542.

Schnegg P.-A., 2003. A new field fluorometer for multi-tracer tests and turbidity measurement applied to hydrogeological problems. Proceedings of the Eight International Congress of the Brazilian Geophysical Society, Rio de Janeiro.

Tritz S., Guinot V., & Jourde H., 2011. Modelling the behaviour of a karst system catchment using non-linear hysteretic conceptual model, *Journal of Hydrology*, 397:250-262.